RESEARCH ARTICLE

WILEY

Monitoring ecosystem service change in the City of Shenzhen by the use of high-resolution remotely sensed imagery and deep learning

Xin Huang[1,2] | Xiaopeng Han[2] | Song Ma[3] | Tianjia Lin[3] | Jianya Gong[1]

[1] School of Remote Sensing and Information Engineering, Wuhan University, Wuhan 430079, PR China

[2] System Research Department, The 14th Research Institute of China Electronics Technology Group Corporation, Nanjing 210039, PR China

[3] Shenzhen Environmental Monitoring Centre, Shenzhen 518049, PR China

Correspondence
Xin Huang, School of Remote Sensing and Information Engineering, Wuhan University, Wuhan 430079, PR China.
Email: xhuang@whu.edu.cn; huang_whu@163.com

Abstract

Information concerning land-use change is imperative for improving conservation policies that promote sustainable land development. However, to date, most of the previous studies have largely focused on the use of coarse- or moderate-resolution data, with which it may not be possible to identify the land-use classes in urban environments. Due to the improved spatial details, high-resolution (HR) remote sensing imagery provides us with an opportunity for the semantic interpretation of urban landscapes. Therefore, in this study, we took the City of Shenzhen (1997 km^2) in China as an example to assess the detailed land-use change and its effect on ecosystem services (ESs), based on HR satellite data from 2005 to 2017. In particular, deep learning was used to obtain accurate land-use maps, because this technique is able to model the hierarchical representations of features and can thus effectively characterize urban scenes. The results revealed the following findings: (a) The overall accuracy of the proposed approach was 96.9% and 97.1% for 2005 and 2017, respectively, outperforming state-of-the-art semantic classification models; (b) residential and commercial areas in Shenzhen increased dramatically over the study period by 10,416 and 9,168 ha, at the expense of ecological land; (c) supply capacity of the ecosystem decreased by 13.7%, but demand for ESs showed an increase of 23.5%. By courtesy of HR images, detailed land-use changes and the associated ESs can be monitored, which facilitates the in-depth understanding of urban environmental systems.

KEYWORDS

ecosystem service, land degradation, land-use development, urban environment, urbanization

1 | INTRODUCTION

Rapid urban development is having an increasingly strong negative impact on the Earth's environment, causing, for example, land degradation, resource depletion, and other environmental problems (Çakir et al., 2008; Chuai et al., 2018). Ecosystem services (ESs) are a concept that can express the condition and quality of the natural environment, for which the provision of services depends on the biophysical conditions and their changes over space and time (Mamat, Halik, Keyimu, Keram, & Nurmamat, 2018). More importantly, ESs have a direct effect on human health and security, such as local climate regulation and flood protection (Zhang, Fu, Zeng, Geng, & Hassani, 2013). Therefore, quantifying and mapping ESs is important to support decision-making on sustainability issues, as well as ecological protection (Sietz, Fleskens, & Stringer, 2017).

To achieve the reliable monitoring of ESs, quick and low-cost approaches are required (Ayanu, Conrad, Nauss, Wegmann, & Koellner, 2012). For this reason, remote sensing techniques have been widely used, due to their broad scale applicability. There are two categories of approaches to map ESs based on remote sensing data. The first approach directly links the radiative signal derived from the remote sensing data to in situ observations, by the use of statistical regression or a radiative transfer model. However, the validity and applicability in other study areas are restricted by many factors, such as the lack of a priori knowledge about phenology and land processes (Krishnaswamy, Bawa, Ganeshaiah, & Kiran, 2009). The second type of method is based on the fact that land-use classes can be used as a proxy for ESs, which has been widely acknowledged as a useful tool for the quantification and mapping of ESs (Ayanu et al., 2012). Specifically, information on ESs can be obtained through land-use classification, in which the derived classes represent or indicate at least one ecosystem function.

Based on these mapping approaches, a large number of studies have shown that undesirable and damaging land-use changes can result in widespread ecosystem degradation (Papanastasis et al., 2015; Zhang, Yu, Li, Zhou, & Zhang, 2006). Ecosystems are often disturbed by human activities and land-use changes, and the capacity to provide services can also be impacted (Foley et al., 2005; Peng, Liu, Li, & Wu, 2017). To achieve balanced and sustainable development of an ecosystem, the supply of ESs should satisfy the demands of human society. Dynamic analysis focusing on ecosystem supply and demand and their budgets is essential for natural resource management and landscape sustainability assessments (Zhang, Peng, Liu, & Wu, 2017). Furthermore, it should be mentioned that different land-use categories have varying magnitudes of ES provision and demand (Burkhard, Kroll, Nedkov, & Müller, 2012). By taking this into account, the detailed distinction of land-use categories might provide more precise information about service provision and demand. However, to the best of our knowledge, there have been few attempts to relate detailed land-use patterns to the quantification of ESs, especially when simultaneously considering ES supply and demand.

Therefore, detailed land-use information is of vital significance for precisely monitoring ecosystems. With the rapid development of space imaging techniques, remote satellite sensors can provide high-resolution (HR) data (Huang et al., 2016; Huang, Wen, Li, & Qin, 2017). For instance, the QuickBird and GaoFen-2 satellites are able to provide multispectral images with 2.4-m and 4-m spatial resolutions. The abundant spatial and structural information of HR images makes it possible to classify remote sensing scenes into detailed land-use classes (Huang, Zhao, & Song, 2018). Recent research in scene classification, in which a scene refers to an image block that belongs to a user-defined semantic category, has shown its potential for the semantic interpretation of remote sensing scenes (Wu, Zhang, & Zhang, 2016). The scene-based approach is able to describe the spatial arrangement of the objects within the scenes as a whole, and is therefore suitable for dealing with complex land-use classes. Although numerous scene-based classification methods have been developed (e.g., the bag-of-visual-words [BOVW] model), they sometimes fail to capture the fine features of complex urban scenes. On the other hand, deep learning has received much attention recently, because it can model the hierarchical representations of the features of pixel intensities, edges, object parts, objects, and land parcels (LeCun, Bengio, & Hinton, 2015). However, the performance of deep learning has not been evaluated for land-use change analysis over a relatively large geographical scale (e.g., the city level), in terms of the efficiency and accuracy in practical applications.

Based on the above considerations, we took the City of Shenzhen in China as an example of an urban area that has suffered from serious conflicts between economic development and ecological protection, and we explored the detailed land-use changes and associated ecosystem degradation in this city between 2005 and 2017. Specifically, in order to obtain accurate land-use maps, the deep learning technique was used for the classification of multitemporal HR images. Subsequently, the ESs and their dynamics were quantified by linkage with the land-use categories. In summary, the objectives of this study were to link detailed land-use classes to ESs by the use of HR satellite images and the deep learning technique, and to comprehensively analyze the long-term land-use changes and ecosystem degradation characteristics in the City of Shenzhen.

2 | MATERIALS AND METHODS

2.1 | Study area

The City of Shenzhen (113°46′–114°37′E, 22°27′–22°52′N), located in Guangdong Province, China, was chosen as the study area, because this city has experienced rapid economic and urban development over the past 40 years (Figure 1). Because Shenzhen became China's first Special Economic Zone in 1979, it has been transformed from an unknown fishing village into one of the largest cities in the Pearl River Delta. During this period, Shenzhen's population has increased from less than 100,000 in 1979 to over 12 million in 2017, accompanied by huge migration from other domestic cities (Shenzhen Statistics Bureau, 2017). Moreover, gross domestic product (GDP) had reached $328.7 billion by 2017 (Shenzhen Statistics Bureau, 2017). With the rapid development, Shenzhen has become a 'window' of China for economic, scientific, and technological exchanges.

Along with the rapid land-use/cover change caused by urbanization, Shenzhen has experienced environmental problems and ecosystem degradation. Unspoiled land, including water bodies, forest, and grassland, has had higher probability of transition to construction land during the urban development (Peng, Zhao, Guo, Pan, & Liu, 2017). Moreover, a significant deterioration of urban ecosystem health during 2000–2005 has been reported in Shenzhen, for which ESs have been the most useful indicator (Peng, Liu, Wu, Lv, & Hu, 2015). In response, the Shenzhen municipal government has begun to implement a series of measures for sustainable land-use development. Thus, research into detailed land-use and ecosystem changes is urgently required for a more complete understanding of the ecosystem degradation characteristics in Shenzhen.
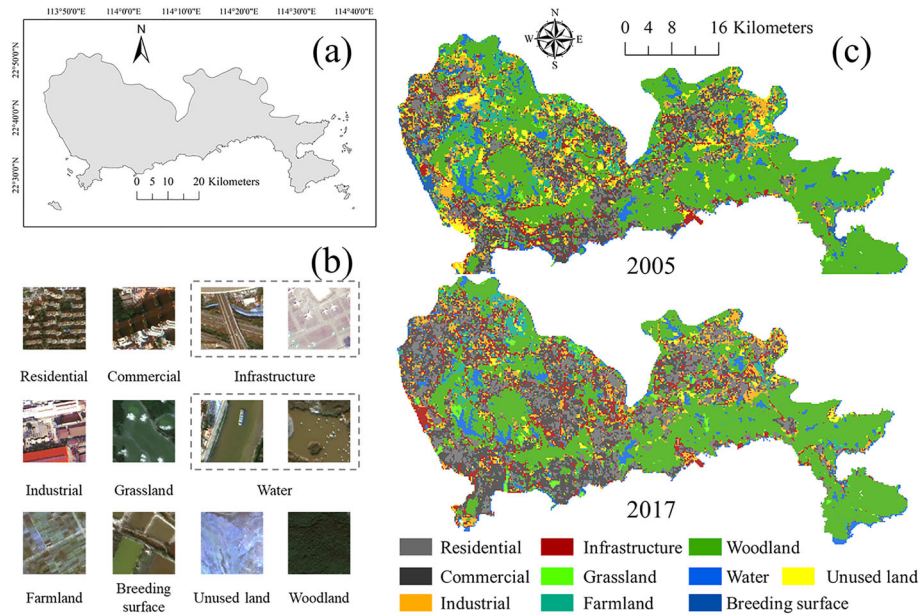
FIGURE 1 Study area and datasets: (a) overview of the study area, (b) samples of each land-use class, and (c) land-use maps for 2005 and 2017 [Colour figure can be viewed at wileyonlinelibrary.com]

2.2 | Data

To assess the detailed land-use patterns in Shenzhen, eight and nine HR satellite images were, respectively, collected to cover the entire city in 2005 and 2017 (referred to as the 'Shenzhen 2005' and 'Shenzhen 2017' images in the following text). In detail, the Shenzhen 2005 and Shenzhen 2017 images were acquired by the QuickBird (2.4-m resolution) and GaoFen-2 (4-m resolution) satellites, respectively. In the image preprocessing step, the raw digital number values of the remote sensing images were converted to surface reflectance using the quick atmospheric correction algorithm (Module, 2009). For the Shenzhen 2017 images, the HR 1-m panchromatic and 4-m multispectral images were fused based on the NNDiffuse pan-sharpening technique (Sun, Chen, & Messinger, 2014), to produce the 1-m multispectral images. The images were stitched together to cover the whole study area, with reflectance correction achieved using histogram matching and edge feathering. Finally, the Shenzhen 2017 and Shenzhen 2005 images were resampled to 2 m for the convenience of analysis and comparison at the same spatial resolution, with the size of 22,950 × 43,769 pixels (i.e., 4,018.0 km^2).

2.3 | Methods

Based on the technical specifications for land-use investigation (China, 2007) and the presence of the prominent land-use types in Shenzhen, 10 classes were defined (Table 1 and Figure 1b). First, multitemporal scene-based classification was conducted, by the use of a transferred deep convolutional neural network (CNN). Subsequently, the land-use change could be identified based on image differencing, and the associated ES information, including both ES supply and demand, could

also be derived by its linkage with the land-use classes. The framework of this study is shown in Figure 2.

2.3.1 | Multitemporal land-use mapping by deep learning

To classify the HR images into different land-use classes, a scene classification method was adopted, that is, a large image was decomposed into a series of nonoverlapped patches or grids as the basic processing units (i.e., scenes), and a class label was assigned to each patch (Huang et al., 2018; Wu et al., 2016). In detail, this method directly characterizes each scene by developing a holistic feature representation, for which the assumption is that the same type of land-use class should share certain characteristics. Therefore, considering the complexity of HR remote sensing images, extracting effective feature descriptors for each scene is the core of the classification task, in order to obtain a satisfactory outcome. The deep learning technique, that is, a CNN, was used in our study, which can effectively model the hierarchical features of urban land-use categories.

In general, the typical architecture of a CNN model includes input, output, and multiple hidden layers, as demonstrated in Figure 3. The hidden layers are typically composed of a number of convolutional, pooling, and fully connected (FC) layers (Zhu et al., 2017). The feature maps of the convolutional layers are extracted by applying a convolution operation to the input image. Each convolutional neuron processes data only for its receptive field. Commonly, an elementwise nonlinear activation function is then applied to these feature maps for a nonlinear transform (e.g., a Rectified Linear Unit). Another important concept of CNNs is pooling, which performs a nonlinear downsampling of the feature maps via average or max pooling. Finally, after several convolutional and pooling layers, FC layers follow as the high-

TABLE 1 Land-use categories and their description in this study

Land-use category	Description	Number of samples (2005)	Number of samples (2017)
Residential	Land use for residential purposes, including urban villages, residential districts, and apartments	340	441
Commercial	Areas, districts, and neighborhoods primarily composed of commercial buildings, such as a central business district and commercial strip	245	428
Industrial	Areas planned for the purpose of industrial development	156	218
Infrastructure	Infrastructure refers to the fundamental facilities and systems, including roads, airports, and container terminals	140	175
Grassland	Grassland in urban parks and golf courses	101	135
Farmland	Irrigated land for cropping	217	111
Water	Rivers, lakes, reservoirs, and so forth	254	298
Breeding	The rearing of aquatic animals or the cultivation of aquatic plants for food	135	49
Woodland	Tree-covered areas	464	687
Unused land	Mainly bare land for construction	170	147
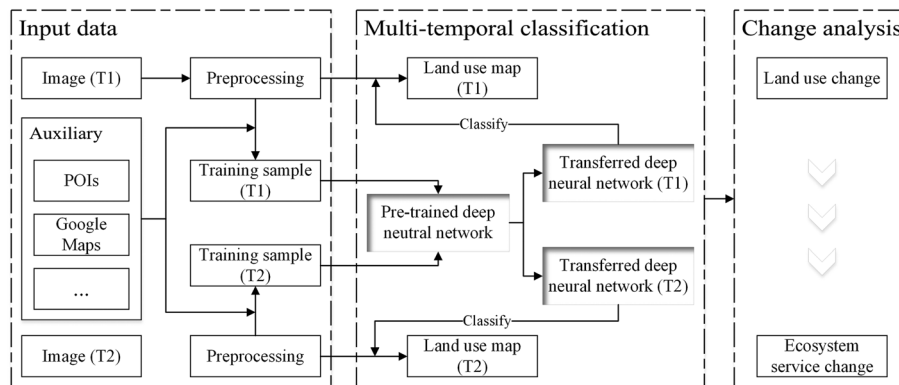
FIGURE 2 Methodology framework

level reasoning parts in the network, where the neurons in an FC layer are connected to all the activations in the previous layer. The last FC layer of the network is a Softmax layer that derives the probability for each land-use class. We refer the interested reader to Goodfellow, Bengio, Courville, and Bengio (2016) for more details about the introduction of CNNs.

However, the number of parameters of the deep CNNs increases significantly with the increase of the number of layers of the network. To reduce the required number of training samples, transferring pre-trained deep CNNs is an alternative approach, which was used in our study. To be specific, a deep CNN was pre-trained with a well-annotated land-use dataset. VGG-VD16 (16 layers; Simonyan & Zisserman, 2014), which is a successful modern CNN architecture, was chosen as the pre-trained model. This model consists of 13 convolutional layers and three FC layers, and it can effectively learn discriminative and powerful image representations and hence improve the classification performance. The labeled scenes, as the target dataset, were then exploited as supervised information for fine-tuning the pre-trained CNN model. Finally, the fine-tuned model was used to classify the HR remote sensing images over the entire city of Shenzhen into land-use maps for the subsequent analysis.

Taking into account both the image resolution and the presence of the dominant land-use classes, which exhibit a variety of scales, we chose 200 m × 200 m as the scene size to characterize the neighborhood extent (i.e., the spatial arrangement and pattern of the land-cover objects; Wu et al., 2016; Xia et al., 2017). It should also be noted that, courtesy of the scene units, that is, grid-cells, with a similar size, the spatial heterogeneity of the ESs can be easily identified (Li, Chen, Wang, & Wang, 2018). The reference samples for each year were independently created by visual inspection and field survey, with the aid of auxiliary data (including point of interest data and Google Earth HR images; Table 1). A random stratification procedure (Schindler,
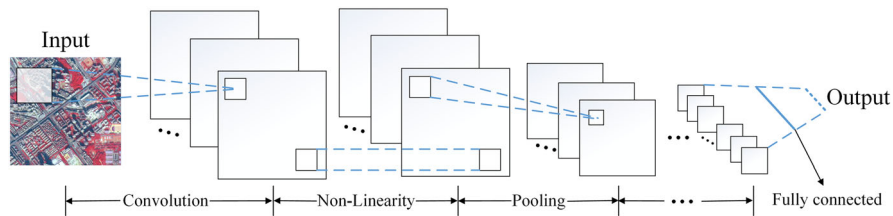
FIGURE 3 Illustration of a typical convolutional neural network architecture [Colour figure can be viewed at wileyonlinelibrary.com]

2012) was then applied to the reference samples to produce disjoint datasets for training (70%) and testing (30%). Finally, the accuracy assessment was performed based on the test dataset.

2.3.2 | ES supply, demand, and budget mapping

Different land-use classes have different ecosystem functions based on their structures and processes. The general assessment approach is based on a matrix that links the different land-use types to ES supply and demand. The values in the matrix are derived by the use of expert evaluation and data from monitoring, measurements, statistics, or interviews (Vihervaara, Kumpula, Tanskanen, & Burkhard, 2010). This method presents a framework to map ES supply, demand, and their budgets, which is both relative and dimensionless (Burkhard et al., 2012).

The supply matrix linking the 10 land-use classes (on the y-axis) and the 22 ESs (on the x-axis) is defined in Table S1. These ESs can represent the main components of the ecosystem functionality (Müller, 2005). The ability of the different land-use classes in unit area (ha) to provide ESs is assessed on a scale of 0 = *no capacity to provide the corresponding ES*; 1 = *low relevant capacity*; 2 = *relevant capacity*; 3 = *medium relevant capacity*; 4 = *high relevant capacity*; and 5 = *very high relevant capacity*.

On the other hand, there must be a certain demand by human society to benefit from a particular ES. The demand matrix illustrating the demand level of the different land-use classes in unit area (ha) for the ESs is given in Table S2 (0 = *no relevant demand*; 1 = *low relevant*

demand; 2 = *relevant demand*; 3 = *medium relevant demand*; 4 = *high relevant demand*; and 5 = *very high relevant demand*).

We computed the budgets by subtracting the demand values from the supply values of each land-use class, to assess the dynamics and flow of goods and services. This information can facilitate the identification of supply–demand mismatches across the area. The budget matrix is defined in Table S3, where the scale ranges from −5 = *strong undersupply*, via 0 = *neutral balance*, to 5 = *strong oversupply*.

It can be seen that many natural or near-natural land-use classes (e.g., woodland, farmland, and water) are characterized by higher supply capability (Table S1), whereas human-dominated urban areas such as residential and commercial areas have higher demand values (Table S2). Furthermore, the pattern in Table S3 indicates that there is an obvious undersupply in the urban area, but an oversupply in the natural and near-natural land-use types. Finally, the spatially explicit information of ES supply, demand, and budget can be derived quantitatively by linking the respective matrix with the land-use maps.

3 | RESULTS

3.1 | Changes of land-use classes

The statistics of the land-use changes are listed in Table 2. It can be clearly seen that the areas (in quantity) of residential, commercial, and infrastructure land have increased significantly. On the one hand, rapid economic development and population growth are the main

TABLE 2 Land-use change from 2005 to 2017

	2005		2017		Change	
Land use	Area (ha)	Percentage (%)	Area (ha)	Percentage (%)	Area (ha)	Change rate (%)
Residential	18,084	9.6	28,500	15.1	10,416	57.6
Commercial	22,828	12.1	31,996	16.9	9,168	40.2
Industrial	16,748	8.9	14,280	7.6	−2,468	−14.7
Infrastructure	11,928	6.3	16,708	8.9	4,780	40.1
Grassland	1,644	0.9	2,860	1.5	1,216	74.0
Farmland	8,384	4.4	6,032	3.2	−2,352	−28.1
Water	9,180	4.9	8,780	4.7	−4,00	−4.4
Breeding surface	3,504	1.8	752	0.4	−2,752	−78.6
Woodland	85,760	45.5	74,136	39.3	−11,624	−13.6
Unused land	10,552	5.6	4,568	2.4	−5,984	−56.7
Total	188,612	100	188,612	100	—	—

Note. Change rate $= \dfrac{\text{Area}(2017) - \text{Area}(2005)}{\text{Area}(2005)} \times 100\%$.

driving forces behind the increase in residential and commercial areas (Bai, 2000; Deng, Fu, & Sun, 2018). For example, from 2005 to 2017, urban per capita disposable income increased from 21,494 Yuan to 52,938 Yuan in Shenzhen. Meanwhile, during this period, Shenzhen's population increased from less than 8.3 million in 2005 to over 12.5 million in 2017 (Shenzhen Statistics Bureau, 2017). On the other hand, according to the "Land Use Planning of Shenzhen City (2006–2020)" document, to accommodate the increasing population with good living conditions, the Urban Planning Land and Resources Commission of Shenzhen Municipality has planned more land and space for housing in the city. The area of residential land increased from 18,084 ha in 2005 to 28,500 ha in 2017 (Table 2). Among the built-up areas (including residential, commercial, industrial, and infrastructure land), residential areas make up 31.2%, which is consistent with the result of Bai (2000). Moreover, the land-use transition is further investigated in Table S4, where it can be seen that most of the residential areas are transformed from commercial, industrial, and woodland.

Relying on the superiority of the geographic location of Shenzhen, that is, the fact that it is adjacent to Hong Kong, and the supporting policy of the special economic zone, Shenzhen's economy has transformed from agriculture to secondary (i.e., heavy industry and construction) and tertiary industries (i.e., services), which has ensured the rapid economic development. It should be noted that the tertiary industries have developed faster in Shenzhen than in other regions, and foreign investment accounts for a large proportion. Under this background, there has been a significant increase in commercial land, with a total area of 9,168 ha (i.e., 40.2% in proportion; Table 2). It can be observed that commercial land accounted for 35.0% of the built-up area in 2017. Again, it has been predicted by Bai (2000) that the proportion of commercial land in the built-up area of Shenzhen will reach 57.0% by 2050, demonstrating the continuing development of commercial land. In this situation, some commercial land has converted from residential land (2,816 ha; Table S4). A typical example of this urban renewal is the redevelopment of urban villages, which are a special informal settlement with substandard living conditions found in cities in China. In addition, based on the "Shenzhen Comprehensive Plan (1996–2010)", the Urban Planning Land and Resources Commission of Shenzhen Municipality has taken active measures to improve the public transport facilities, airports, and parking lots. Between 2005 and 2017, the urban infrastructure of Shenzhen has undergone continuous improvement, with an increase in area of 40.1% (Table 2).

At the same time, it can be observed that secondary industries, that is, industrial land, decreased by 14.7% between 2005 and 2017 (Table 2). In the initial stages of Shenzhen's reform and opening up (1986–1990s), that is, the restructuring phase, secondary industries grew dramatically, contributing to a large proportion of GDP. This process created a large number of employment opportunities. Subsequently, urbanization, referring to the transfer of population to urban areas, continued to accelerate. After long-term development, the industrial structure needs to be adjusted to meet the needs of economic growth. However, with the increase of the urban population and the expansion of the city, land for urban construction has become quite scarce in Shenzhen. In this way, reform and adjustment of the traditional industrial areas has been a priority for the urban development in Shenzhen. The government has paid a lot of attention to optimizing and improving the industrial structure, aiming to develop Shenzhen into an international city with high-efficiency land use (Wang, Lin, & Li, 2010). For example, some buildings in the Dalang industrial area have been transformed into commercial centres since 2008 (Qiu, 2017).

Areas of farmland and breeding surface (areas used for raising aquatic plants and animals) have undergone declines of 28.1% and 78.6%, respectively (Table 2). Accompanying the decrease of these two land-use classes, farmers and rural areas are gradually disappearing in Shenzhen, which demonstrates the transformation process from agricultural village to metropolis. However, the area of breeding surface has declined faster than that of farmland. This is because the Shenzhen municipal government has put farmland protection in a position of high importance, emphasizing its eco-benefits under the background of rapid urbanization. For example, the Shenzhen municipal government has initiated the reclamation of arable land and the establishment of farmland protection areas (Qian, Peng, Luo, Wu, & Du, 2016).

Woodland occupied over 47.0% of the Shenzhen area in 2003 (Mao, Zhigang, Yan, & Zhou, 2008). It has remained the dominant type among all the land-use classes, accounting for 45.5% and 39.3% of the total area in 2005 and 2017, respectively (Table 2). The changes with respect to woodland can be found in Table S4, including its conversion into residential (1,120 ha), commercial (3,648 ha), and industrial areas (2,032 ha). Notably, it can be observed that a large proportion of woodland (4,312 ha) has been converted into infrastructure (e.g., overpasses, airports, and roads). Actually, the shorter the distance to the city center, the higher the transition probability of woodland to public infrastructure tends to become (Peng, Zhao, et al., 2017).

Lastly, unused land, which is mainly an interim form of land use, experienced a sharp decrease of 56.7% from 2005 to 2017. Based on the present situation of land use in the "11th Five-Year Plan for Land Resources Utilization and Protection in Shenzhen," the areas of unused land were 121.9, 118.7, 116.3, 114.5, and 113.5 km^2 in 2000 to 2004, respectively. Based on these results, our study further confirmed that the area of unused land in 2005 was 105.5 km^2, with a decrease of approximately 8.0 km^2 from 2004 to 2005. However, there was only 45.7 km^2 of unused land remaining in 2017, and most of the unused land has been put into reasonable use (e.g., building construction). As noted in the "Land Use Planning of Shenzhen City (2006–2020)" document, the fraction of unused land in Shenzhen is now about 2.2%. This was confirmed in our experimental results, with 2.4% in 2017, highlighting the shortage of land resources for urban development. From 2005 to 2017, most of the unused land has been transformed into commercial (3,636 ha), infrastructure (1,964 ha), and residential areas (908 ha; Table S4). Simultaneously, it should be noted that the transition from unused land to woodland also occupies a large area (1,168 ha). This phenomenon is supported by the land-use policy issued in the "Management Stipulation of the Basic Ecological Line in Shenzhen City," which strictly controls the land-use

development within the basic ecological line. Moreover, it is planned that construction land within the ecological line, which can be considered as environmentally unfriendly, be returned to ecological land, such as grassland, forest, and water bodies, to address the sustainability issues (Bai et al., 2018).

3.2 | Changes of ESs

By linking the land-use maps to the value coefficients of the supply matrix (Table S1), the ES supply and its dynamics can be quantified (Tables 3 and 4(a)). From 2005 to 2017, the total supply values decreased by 13.7%. Due to the larger areas and value coefficients in the supply matrix, the supply capacity of woodland is the highest among all the land-use classes, accounting for 88.5% and 88.4% of the total values in 2005 and 2017, respectively, which is followed by the supply capacity of water bodies, occupying 4.3% and 4.4% in 2005 and 2017, respectively. It can be observed that there have been significant decreases in most of the ESs. Among the ESs in descending order by the supply loss (in proportion), the first three are 'aquaculture,' 'freshwater,' and 'commercial fisheries,' with decreases of 43.0%, 28.8%, and 28.8%, respectively. This phenomenon has mainly been caused by the reduction of farmland and breeding surface, under the process of rapid urbanization in Shenzhen.

ES demands and their dynamics are demonstrated in Tables 3 and 4(b). In general, the total demand values have increased by 23.5%, corresponding to the rapid expansion of human-dominated land-use types (residential, commercial, and infrastructure). Each ES has shown a rising trend in demand because there must be necessary ES demands by human well-being for consuming. Residential, commercial, industrial, and infrastructure areas have relatively high ES demands, occupying 23.0%, 32.7%, 24.0%, and 9.3% of the total demand values in 2005, and 29.4%, 37.1%, 16.6%, and 10.6% in 2017, respectively. Among the ESs in descending order by the demand increase (in proportion), the first five are aquaculture, 'recreation and aesthetic values,' 'livestock,' 'local climate regulation,' and commercial fisheries,

with increases of 32.4%, 31.7%, 30.7%, 30.3%, and 29.6%, respectively. It can be inferred that, along with the urban development, there is a higher requirement for the improvement of the living environment and the availability of ecosystem goods and services.

The information concerning the budgets and their dynamics of matching ES supply and demand is derived from Tables 3 and 4c. In 2005, the total budget value was estimated to be 614,564, which indicates that the ecosystem has enough supply ability to meet the demands of human well-being. However, this value dropped to −1,812,238 in 2017, which shows that demand clearly exceeded supply. There are seven services with supply exceeding demand in both years: 'local climate regulation' 'erosion regulation,' 'nutrient regulation,' 'water purification,' 'pollination,' recreation and aesthetic values, and 'intrinsic value of biodiversity.' Taking this into consideration, we further investigated the temporal dynamics of these seven services (Figure 4). It can be seen that the difference between supply and demand is becoming smaller from 2005 to 2017, indicating degradation of the ecosystem.

4 | DISCUSSION

4.1 | Evaluation of the deep learning technique for land-use mapping

In order to evaluate the effectiveness of the deep learning technique, its performance was compared with the state-of-the-art classification model, that is, BOVW (Yang & Newsam, 2010). In our tests, three commonly used local descriptors, that is, the color histogram (Swain & Ballard, 1991), local binary patterns (Ojala, Pietikainen, & Maenpaa, 2002), and scale-invariant feature transform (Lowe, 2004), were considered as the input features of the standard BOVW model. The experimental results show that deep learning achieves a much better performance than the other methods (Figure 5), which can be attributed to the fact that it has great potential to learn highly discriminative

TABLE 3 Ecosystem service supply, demand, and budget dynamics of each land-use class

Land use	Supply (%)		Demand (%)		Budgets (supply−demand)	
	2005	2017	2005	2017	2005	2017
Residential	18,096 (0.3)	28,520 (0.5)	1,447,680 (23.0)	2,281,600 (29.4)	−1,429,584	−2,253,080
Commercial	22,848 (0.3)	32,020 (0.6)	2,056,320 (32.7)	2,881,796 (37.1)	−2,033,472	−2,849,776
Industrial	16,828 (0.2)	14,312 (0.2)	1,514,513 (24.0)	1,288,076 (16.6)	−1,497,685	−1,273,764
Infrastructure	59,780 (0.9)	84,360 (1.4)	585,842 (9.3)	826,726 (10.6)	−526,062	−742,366
Grassland	54,516 (0.8)	94,644 (1.6)	26,432 (0.4)	45,888 (0.6)	28,084	48,756
Farmland	210,300 (3.0)	150,900 (2.5)	168,240 (2.7)	120,720 (1.6)	42,060	30,180
Water	295,318 (4.3)	263,520 (4.4)	9,844 (0.2)	8,784 (0.1)	285,474	254,736
Breeding surface	118,001 (1.7)	25,344 (0.4)	3,576 (0.1)	768 (0.0)	114,426	24,576
Woodland	6,111,396 (88.5)	5,267,064 (88.4)	258,228 (4.1)	222,552 (2.8)	5,853,168	5,044,512
Unused land	0 (0)	0 (0)	221,844 (3.5)	96,011 (1.2)	−221,844	−96,011
Total	6,907,083 (100)	5,960,684 (100)	6,292,519 (100)	7,772,922 (100)	614,564	−1,812,238

TABLE 4 Ecosystem service (ES) dynamics of (a) supply; (b) demand; and (c) their budgets (ESs with supply exceeding demand in both years are highlighted in bold)

		1	2	3	4	5	6	7	8	9	10	11
(a) Supply	2005	477,347	371,092	317,580	209,055	438,792	447,052	452,060	438,640	430,380	42,060	47,016
	2017	407,832	320,928	291,624	176,376	376,956	391,296	394,812	385,260	370,920	30,180	38,784
	Change (%)	−14.6	−13.5	−8.2	−15.6	−14.1	−12.5	−12.7	−12.2	−13.8	−28.3	−17.5
(b) Demand	2005	186,912	308,903	308,452	310,880	357,311	123,180	200,312	175,076	245,076	322,836	314,424
	2017	243,592	390,743	382,075	400,036	455,223	140,648	206,840	188,732	305,568	416,908	410,872
	Change (%)	30.3	26.5	23.9	28.7	27.4	14.2	3.3	7.8	24.7	29.1	30.7
(c) Budgets	2005	290,436	62,188	9,128	−101,824	81,481	323,872	251,748	263,564	185,304	−280,776	−267,408
	2017	164,240	−69,815	−90,452	−223,660	−78,267	250,648	187,972	196,528	65,352	−386,728	−372,088

Note. Ecosystem services: **1, local climate regulation; 2, global climate regulation; 3, flood protection; 4, groundwater recharge; 5, air quality regulation; 6, erosion regulation; 7, nutrient regulation; 8, water purification; 9, pollination;** 10, crops; 11, livestock; 12, fodder; 13, commercial fisheries; 14, aquaculture; 15, wild foods; 16, timber; 17, wood fuel; 18, energy; 19, biochemicals and medicine; 20, freshwater; 21, recreation and aesthetic values; **22, intrinsic value of biodiversity.**

TABLE 4 (continued)

		12	13	14	15	16	17	18	19	20	21	22
(a) Supply	2005	128,136	40,259	37,567	487,363	430,380	430,380	164,216	438,792	67,099	522,803	489,015
	2017	104,364	28,656	21,408	414,864	370,920	370,920	171,944	376,956	47,760	450,192	417,732
	Change (%)	−18.6	−28.8	−43.0	−14.9	−13.8	−13.8	4.7	−14.1	−28.8	−13.9	−14.6
(b) Demand	2005	240,388	286,515	273,096	347,216	440,779	344,560	409,371	309,228	357,571	261,608	168,828
	2017	293,924	371,224	361,672	418,984	494,051	396,628	491,847	397,168	445,791	344,624	215,775
	Change (%)	22.3	29.6	32.4	20.7	12.1	15.1	20.2	28.4	24.7	31.7	27.8
(c) Budgets	2005	−112,252	−246,256	−235,529	140,147	−10,399	85,820	−245,156	129,564	−290,473	261,195	320,187
	2017	−189,560	−342,568	−340,264	−4,120	−123,131	−25,708	−319,903	−20,212	−398,031	105,568	201,956
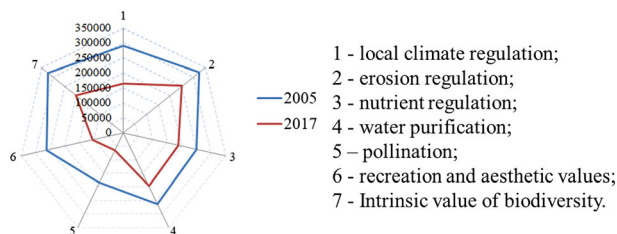
FIGURE 4 Spider chart illustrating the temporal dynamics of the seven ecosystem services with supply exceeding demand [Colour figure can be viewed at wileyonlinelibrary.com]
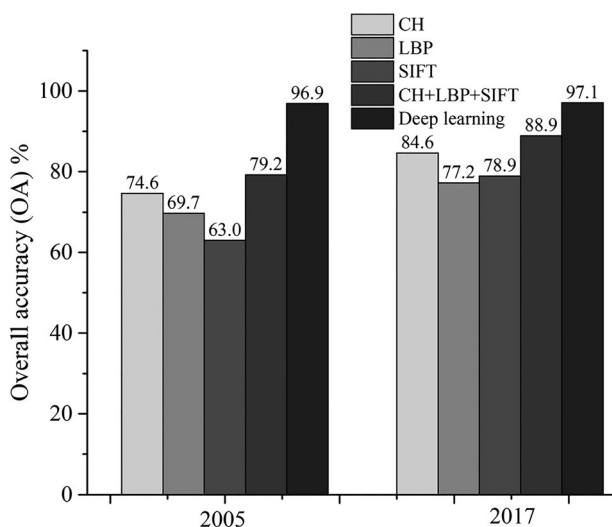
FIGURE 5 Comparison between the different scene classification methods

features with the deep architecture. To be specific, due to the large variations in the spatial arrangements of land-use classes, it is difficult for the BOVW model to effectively capture the fine features of complex image scenes. However, because deep learning adopts a multi-stage global feature learning architecture to adaptively learn image features, and casts the scene classification as an end-to-end problem (Xia et al., 2017; Zhu et al., 2017), it can exploit the intrinsic characteristic of satellite images and achieve a far better classification performance. The overall accuracies are 96.9% and 97.1% for 2005 and 2017, respectively, indicating that the deep learning technique can produce reliable land-use maps for monitoring urban ESs.

4.2 | Ecological and environmental problems caused by rapid land-use change

Over the past 40 years, Shenzhen has transformed from a small village into one of the largest cities in China. It should be mentioned that, despite the rapid economic development, the fragile ecosystem in Shenzhen experienced degradation along with the process of intensive land-use changes (Peng et al., 2015; Su, Xiao, Jiang, & Zhang, 2012). From 2005 to 2017, residential and commercial areas increased by 57.6% and 40.2%, respectively (Table 2). This raises the question of

how to dispose of domestic garbage and sewage (Chen, Jiao, Huang, & Huang, 2007). For instance, domestic garbage increased from 4.57 to 6.03 million tons, and domestic sewage increased dramatically from 640 to 1392 million tons from 2005 to 2017 (Human Settlements and Environment Commission of Shenzhen Municipality, 2017). Improper disposal of these wastes results in deterioration of the ecological environment and its services, and this trend is being intensified (Abulizi et al., 2016; Wang et al., 2017). According to the "China Sustainable Cities Report" (2016), the City of Shenzhen ranks 19 out of the 35 large- and medium-sized cities in China in terms of the water pollutant discharge indicator and is 30th for the solid water discharge indicator.

Moreover, in response to land-use changes, ES demand from human well-being has obviously exceeded the supply capacity of the ecosystem from 2005 to 2017 in Shenzhen, which indicates ecosystem degradation (Table 4 and Figure 4). This phenomenon is also supported by the findings of a study, which focused on ecosystem health and its economic value in Shenzhen (Li, Li, & Qian, 2010). To be specific, with the increase of residential, commercial, and infrastructure land, there is a higher demand for ESs, in terms of provisioning services of material or energy, cultural services comprising recreation and aesthetic values, and regulating services that control the quality of the living environment (with an increase of 23.5%). However, due to the decline of ecological land, the ES supply capacity of the ecosystem decreased by 13.7% from 2005 to 2017. For example, air quality during 2017 was worse than that during 2016 in Shenzhen. Inhalable particle and fine particle concentrations have increased by 3 and 1 μg m^{-3}, respectively (Human Settlements and Environment Commission of Shenzhen Municipality, 2017). Several natural or near-natural land-use classes (e.g., woodland) that are characterized by a higher supply capacity of air quality regulation have also declined significantly. These findings should raise concern for the protection of the ecological environment.

As mentioned above, rapid urbanization has created a high demand for land resources, and the municipal government is now faced with a land crisis (Grimm et al., 2008; Peng et al., 2017). After a period of overexploitation of land, there has been extensive land reclamation from the sea in Shenzhen over the past few decades. Furthermore, 90% of the coastal zone is also impacted by human activities, which has resulted in severe wetland degradation. The "Land Use Planning of Shenzhen City (2006–2020)" document reports that the mangrove forest and coastal shoals have experienced a sharp shrinkage of about 70% and 72%, respectively, due to the excessive pursuit of more land resources. There is no doubt that these changes have had a negative effect on the ecosystem (Wolters, Gillis, Bouma, Katwijk, & Ziegler, 2015).

4.3 | Land policies to promote sustainable urban development

As previously mentioned, the scarcity of land resources for urban development in Shenzhen is a serious challenge, because a large volume of land resources has been consumed after the long period

of land development in this city (Qian et al., 2016). As indicated in our study, even unused land, however, experienced a sharp decrease of 56.7% from 2005 to 2017 (Table 2). Therefore, the government issued the "Management Stipulation of the Basic Ecological Line in Shenzhen City" in 2005, aiming to strictly control land-use development within the basic ecological line. However, land sources outside the ecological line are gradually declining with the continuous expansion of built-up areas. Moreover, there is still room for improving the land-use efficiency in Shenzhen. For instance, the average GDP per area of Shenzhen was 400 million Yuan per km^2 in 2008, which was only 28% of that in Singapore. At the same time, it has been reported that the ES values of Shenzhen only made up about 2.9% of GDP in 1996, 0.9% in 2000, and 0.7% in 2004, showing a decreasing trend (Li et al., 2010). For efficient utilization of land resources, rational land-use planning and policies should play an important role in Shenzhen's sustainable urban development.

On the one hand, in order to reduce the conversion from ecological land to urban land, the Shenzhen municipal government has mitigated the dependence on land finances (Tian, 2015). As mentioned above, after the establishment of the basic ecological line, the urban growth boundary has also been delineated, within which land-use development is strictly controlled for ecological protection. Furthermore, arable land reclamation and farmland protection have been conducted in Shenzhen since 2012, aiming to address the loss of farmland and improve the ecological quality of the local environment. The ecological benefits of arable land are far more valuable than its food supply function and, therefore, the Shenzhen municipal government has put farmland protection in the position of high importance. Actually, both breeding surface and farmland are agriculture-related land-use classes for Shenzhen, but the ecological benefits of breeding surface need further study when incorporating environmental issues into development decisions.

To balance urban development and ecological conservation, more effective actions are required. In this regard, the Human Settlements and Environment Commission of Shenzhen Municipality, an official environmental management department of China, has begun to determine ecological redline areas (ERAs) since 2018. China's ecological redline policy (ERP) is one of the first national policies incorporating multiple ESs into development decisions, which prescribes a stricter control of land-use development within the ERAs for the protection of key ecological function zones (Bai et al., 2018). However, there is no standardized method for determining ERAs to promote effective decision-making. Our study presents a framework integrating land-use classification and ES assessment, which could provide policymakers with the essential information for urban planning.

4.4 | Limitations and future work

The basic idea of this study was that different land-use types are linked to different capacities to provide or consume various ESs (Maes et al., 2012). The assignments in the matrices were first based on expert evaluation from different case-studies and could be further adjusted when additional data measurements, modeling, or expert assessments are available (Burkhard et al., 2012). However, ES supply and demand matrices have not been localized for Shenzhen. Therefore, research into the localization of the ES supply and demand matrices for Chinese cities is suggested to obtain more accurate assessment and mapping of ESs. In addition, with the aid of HR satellite data, the ES supply and demand for other cities in China could be quantified, which would facilitate more general and in-depth analysis. Finally, with the development of remote sensing imaging techniques, we will be able to monitor ES dynamics with dense time series (or a high temporal resolution), achieving a better understanding of the changing process.

5 | CONCLUSIONS

The availability of HR remote sensing imagery, which contains detailed ground information, has opened new avenues for remote sensing applications. In this study, inspired by this fact, we investigated the potential of HR images for land-use mapping and ES monitoring. However, there is a huge semantic gap between remote sensing data and land-use categories. Deep learning can effectively bridge this gap, courtesy of its ability to extract discriminative features from the original pixel values of satellite images. In this way, the detailed land-use changes and ecosystem degradation could be explored for Shenzhen for the period of 2005 to 2017. The conclusions of this study are summarized as follows.

1. Compared with the state-of-the-art semantic classification models (e.g., BOVW), the deep learning technique is more appropriate for classifying remote sensing scenes into land-use classes, with the overall accuracy being 96.9% and 97.1% for 2005 and 2017, respectively. The combined use of HR images and the deep learning technique can facilitate the accurate monitoring of land-use and ecosystem dynamics.

2. Supply capacity of the ecosystem has decreased by 13.7%, due to the area reductions of woodland, water, farmland, and so forth. On the other hand, ES demand from human well-being has shown a significant increase of 23.5%, which can be attributed to the urban development and the expansion of residential, commercial, and infrastructure land. This phenomenon of ES demand clearly exceeding supply implies overexploitation, and thus degradation, of the ecosystem in Shenzhen.

3. In response to the ecosystem degradation, more effective measures, such as ERP, should be taken. This study could help to present a framework for developing Shenzhen's ERP using ES assessments. It should be noted that Shenzhen, and even the whole of China, has promoted the coordinated development of the ecology, the economy, and society in order to relieve the pressures on ESs, and thus achieve sustainable goals.

REFERENCES

Abulizi, A., Yang, Y., Mamat, Z., Luo, J., Abdulslam, D., Xu, Z., ... Halik, W. (2016). Land-use change and its effects in Charchan Oasis, Xinjiang, China. *Land Degradation & Development*, 28(1), 106–115. https://doi.org/10.1002/ldr.2530

Ayanu, Y. Z., Conrad, C., Nauss, T., Wegmann, M., & Koellner, T. (2012). Quantifying and mapping ecosystem services supplies and demands: A review of remote sensing applications. *Environmental Science & Technology*, 46(16), 8529–8541. https://doi.org/10.1021/es300157u

Bai, W. Q. (2000). Analysis on land use dynamics of Shenzhen. *Journal of Natural Resources*, 15(2), 112–116. https://doi.org/10.11849/zrzyxb.2000.02.003

Bai, Y., Wong, C. P., Jiang, B., Hughes, A. C., Wang, M., & Wang, Q. (2018). Developing China's Ecological Redline Policy using ecosystem services assessments for land use planning. *Nature Communications*, 9(1), 3034. https://doi.org/10.1038/s41467-018-05306-1

Burkhard, B., Kroll, F., Nedkov, S., & Müller, F. (2012). Mapping ecosystem service supply, demand and budgets. *Ecological Indicators*, 21, 17–29. https://doi.org/10.1016/j.ecolind.2011.06.019

Çakir, G., Ün, C., Baskent, E. Z., Köse, S., Sivrikaya, F., & Keleş, S. (2008). Evaluating urbanization, fragmentation and land use/land cover change pattern in Istanbul city, Turkey from 1971 to 2002. *Land Degradation & Development*, 19(6), 663–675. https://doi.org/10.1002/ldr.859

Chen, K., Jiao, J. J., Huang, J., & Huang, R. (2007). Multivariate statistical evaluation of trace elements in groundwater in a coastal area in Shenzhen, China. *Environmental Pollution*, 147(3), 771–780. https://doi.org/10.1016/j.envpol.2006.09.002

China, M. o. N. R. o. t. P. s. R. o. (2007). Technical Specification for Updating the Second National Land Survey Database. China environmental press retrieved from http://www.mlr.gov.cn/wszb/2009/20090612qmpxxxgtzygb_1_2/beijingziliao/200911/t20091127_697570.htm.

China Sustainable Cities Report. (2016). China sustainable cities Report 2016: Measuring ecological input and human development.

Chuai, X., Qi, X., Zhang, X., Li, J., Yuan, Y., Guo, X., ... Lv, X. (2018). Land degradation monitoring using terrestrial ecosystem carbon sinks/sources and their response to climate change in China. *Land Degradation & Development*, 29(10), 3489–3502. https://doi.org/10.1002/ldr.3117

Deng, Y., Fu, B., & Sun, C. (2018). Effects of urban planning in guiding urban growth: Evidence from Shenzhen, China. *Cities*, 83, 118–128. https://doi.org/10.1016/j.cities.2018.06.014

Goodfellow, I., Bengio, Y., Courville, A., & Bengio, Y. (2016). *Deep learning* (Vol. 1). Cambridge: MIT press.

Grimm, N. B., Foster, D., Groffman, P., Grove, J. M., Hopkinson, C. S., Nadelhoffer, K. J., ... Peters, D. P. C. (2008). The changing landscape: Ecosystem responses to urbanization and pollution across climatic and societal gradients. *Frontiers in Ecology and the Environment*, 6(5), 264–272. https://doi.org/10.1890/070147

Huang, B., Zhao, B., & Song, Y. (2018). Urban land-use mapping using a deep convolutional neural network with high spatial resolution multispectral remote sensing imagery. *Remote Sensing of Environment*, 214, 73–86. https://doi.org/10.1016/j.rse.2018.04.050

Huang, X., Han, X., Zhang, L., Gong, J., Liao, W., & Benediktsson, J. A. (2016). Generalized differential morphological profiles for remote sensing image classification. *IEEE Journal of Selected Topics in Applied Earth Observations and Remote Sensing*, 9(4), 1736–1751. https://doi.org/10.1109/JSTARS.2016.2524586

Huang, X., Wen, D., Li, J., & Qin, R. (2017). Multi-level monitoring of subtle urban changes for the megacities of China using high-resolution multi-view satellite imagery. *Remote Sensing of Environment*, 196, 56–75. https://doi.org/10.1016/j.rse.2017.05.001

Human Settlements and Environment Commission of Shenzhen Municipality. (2017). Shenzhen Environmental Quality Reports.

Krishnaswamy, J., Bawa, K. S., Ganeshaiah, K. N., & Kiran, M. C. (2009). Quantifying and mapping biodiversity and ecosystem services: Utility of a multi-season NDVI based Mahalanobis distance surrogate. *Remote Sensing of Environment*, 113(4), 857–867. https://doi.org/10.1016/j.rse.2008.12.011

LeCun, Y., Bengio, Y., & Hinton, G. (2015). Deep learning. *Nature*, 521, 436–444. https://doi.org/10.1038/nature14539

Li, B., Chen, N., Wang, Y., & Wang, W. (2018). Spatio-temporal quantification of the trade-offs and synergies among ecosystem services based on grid-cells: A case study of Guanzhong Basin, NW China. *Ecological Indicators*, 94, 246–253. https://doi.org/10.1016/j.ecolind.2018.06.069

Li, T., Li, W., & Qian, Z. (2010). Variations in ecosystem service value in response to land use changes in Shenzhen. *Ecological Economics*, 69(7), 1427–1435. https://doi.org/10.1016/j.ecolecon.2008.05.018

Lowe, D. G. (2004). Distinctive image features from scale-invariant keypoints. *International Journal of Computer Vision*, 60(2), 91–110. https://doi.org/10.1023/B:VISI.0000029664.99615.94

Maes, J., Egoh, B., Willemen, L., Liquete, C., Vihervaara, P., Schägner, J. P., ... Bidoglio, G. (2012). Mapping ecosystem services for policy support and decision making in the European Union. *Ecosystem Services*, 1(1), 31–39. https://doi.org/10.1016/j.ecoser.2012.06.004

Mamat, Z., Halik, Ü., Keyimu, M., Keram, A., & Nurmamat, K. (2018). Variation of the floodplain forest ecosystem service value in the lower reaches of Tarim River, China. *Land Degradation & Development*, 29(1), 47–57. https://doi.org/10.1002/ldr.2835

Mao, J. X., Zhigang, L. I., Yan, X. P., & Zhou, S. H. (2008). Human dimensions of land use change in the context of rapid urbanization in Shenzhen. *Resources Science*, 30(6), 939–948. https://doi.org/10.3321/j.issn:1007-7588.2008.06.021

Module, F. (2009). Atmospheric correction module: QUAC and FLAASH user's guide. Version, 4, 44.

Müller, F. (2005). Indicating ecosystem and landscape organisation. *Ecological Indicators*, 5(4), 280–294. https://doi.org/10.1016/j.ecolind.2005.03.017

Ojala, T., Pietikainen, M., & Maenpaa, T. (2002). Multiresolution gray-scale and rotation invariant texture classification with local binary patterns. *IEEE Transactions on Pattern Analysis and Machine Intelligence*, 24(7), 971–987. https://doi.org/10.1109/TPAMI.2002.1017623

Papanastasis, V. P., Bautista, S., Chouvardas, D., Mantzanas, K., Papadimitriou, M., Mayor, A. G., ... Vallejo, R. V. (2015). Comparative assessment of goods and services provided by grazing regulation and reforestation in degraded Mediterranean rangelands. *Land Degradation & Development*, 28(4), 1178–1187. https://doi.org/10.1002/ldr.2368

Peng, J., Liu, Y., Li, T., & Wu, J. (2017). Regional ecosystem health response to rural land use change: A case study in Lijiang City, China. *Ecological Indicators*, 72, 399–410. https://doi.org/10.1016/j.ecolind.2016.08.024

Peng, J., Liu, Y., Wu, J., Lv, H., & Hu, X. (2015). Linking ecosystem services and landscape patterns to assess urban ecosystem health: A case study in Shenzhen City, China. *Landscape and Urban Planning*, 143, 56–68. https://doi.org/10.1016/j.landurbplan.2015.06.007

Peng, J., Tian, L., Liu, Y., Zhao, M., Hu, Y. n., & Wu, J. (2017). Ecosystem services response to urbanization in metropolitan areas: Thresholds

identification. *Science of the Total Environment*, *607-608*, 706–714. https://doi.org/10.1016/j.scitotenv.2017.06.218

Peng, J., Zhao, M., Guo, X., Pan, Y., & Liu, Y. (2017). Spatial-temporal dynamics and associated driving forces of urban ecological land: A case study in Shenzhen City, China. *Habitat International*, *60*, 81–90. https://doi.org/10.1016/j.habitatint.2016.12.005

Qian, J., Peng, Y., Luo, C., Wu, C., & Du, Q. (2016). Urban land expansion and sustainable land use policy in Shenzhen: A case study of China's rapid urbanization. *Sustainability*, *8*(1), 1–16 https://doi.org/10.3390/su8010016

Qiu, C. (2017). from https://city.shenchuang.com/szcsjg/20170407/439953_2.shtml

Schindler, K. (2012). An overview and comparison of smooth labeling methods for land-cover classification. *IEEE Transactions on Geoscience and Remote Sensing*, *50*(11), 4534–4545. https://doi.org/10.1109/TGRS.2012.2192741

Shenzhen Statistics Bureau (2017). *Shenzhen statistical yearbook*. Beijing: China Statistics Press.

Sietz, D., Fleskens, L., & Stringer, L. C. (2017). Learning from non-linear ecosystem dynamics is vital for achieving land degradation neutrality. *Land Degradation & Development*, *28*(7), 2308–2314. https://doi.org/10.1002/ldr.2732

Simonyan, K., & Zisserman, A. (2014). Very deep convolutional networks for large-scale image recognition. *arXiv preprint arXiv:1409.1556*.

Su, S., Xiao, R., Jiang, Z., & Zhang, Y. (2012). Characterizing landscape pattern and ecosystem service value changes for urbanization impacts at an eco-regional scale. *Applied Geography*, *34*, 295–305. https://doi.org/10.1016/j.apgeog.2011.12.001

Sun, W., Chen, B., & Messinger, D. (2014). Nearest-neighbor diffusion-based pan-sharpening algorithm for spectral images. *Optical Engineering*, *53*(1), 013107. https://doi.org/10.1117/1.OE.53.1.013107

Swain, M. J., & Ballard, D. H. (1991). Color indexing. *International Journal of Computer Vision*, *7*(1), 11–32. https://doi.org/10.1007/BF00130487

Tian, L. (2015). Land use dynamics driven by rural industrialization and land finance in the peri-urban areas of China: "The examples of Jiangyin and Shunde". *Land Use Policy*, *45*, 117–127. https://doi.org/10.1016/j.landusepol.2015.01.006

Vihervaara, P., Kumpula, T., Tanskanen, A., & Burkhard, B. (2010). Ecosystem services—A tool for sustainable management of human–environment systems. Case study Finnish Forest Lapland. *Ecological Complexity*, *7*(3), 410–420. https://doi.org/10.1016/j.ecocom.2009.12.002

Wang, C. C., Lin, G. C. S., & Li, G. (2010). Industrial clustering and technological innovation in China: New evidence from the ICT industry in Shenzhen. *Environment and Planning a: Economy and Space*, *42*(8), 1987–2010. https://doi.org/10.1068/a4356

Wang, J., Lin, Y., Zhai, T., He, T., Qi, Y., Jin, Z., & Cai, Y. (2017). The role of human activity in decreasing ecologically sound land use in China. *Land Degradation & Development*, *29*(3), 446–460. https://doi.org/10.1002/ldr.2874

Wolters, J.-W., Gillis, L. G., Bouma, T. J., Katwijk, M. M., & Ziegler, A. D. (2015). Land use effects on mangrove nutrient status in Phang Nga Bay, Thailand. *Land Degradation & Development*, *27*(1), 68–76. https://doi.org/10.1002/ldr.2430

Wu, C., Zhang, L., & Zhang, L. (2016). A scene change detection framework for multi-temporal very high resolution remote sensing images. *Signal Processing*, *124*, 184–197. https://doi.org/10.1016/j.sigpro.2015.09.020

Xia, G., Hu, J., Hu, F., Shi, B., Bai, X., Zhong, Y., ... Lu, X. (2017). AID: A benchmark data set for performance evaluation of aerial scene classification. *IEEE Transactions on Geoscience and Remote Sensing*, *55*(7), 3965–3981. https://doi.org/10.1109/TGRS.2017.2685945

Yang, Y., & Newsam, S. (2010). Bag-of-visual-words and spatial extensions for land-use classification. Paper presented at the Proceedings of the 18th SIGSPATIAL international conference on advances in geographic information systems: California, USA

Zhang, J. J., Fu, M. C., Zeng, H., Geng, Y. H., & Hassani, F. P. (2013). Variations in ecosystem service values and local economy in response to land use: A case study of Wu'an, China. *Land Degradation & Development*, *24*(3), 236–249. https://doi.org/10.1002/ldr.1120

Zhang, K., Yu, Z., Li, X., Zhou, W., & Zhang, D. (2006). Land use change and land degradation in China from 1991 to 2001. *Land Degradation & Development*, *18*(2), 209–219. https://doi.org/10.1002/ldr.757

Zhang, L., Peng, J., Liu, Y., & Wu, J. (2017). Coupling ecosystem services supply and human ecological demand to identify landscape ecological security pattern: A case study in Beijing–Tianjin–Hebei region, China. *Urban Ecosystems*, *20*(3), 701–714. https://doi.org/10.1007/s11252-016-0629-y

Zhu, X. X., Tuia, D., Mou, L., Xia, G., Zhang, L., Xu, F., & Fraundorfer, F. (2017). Deep learning in remote sensing: A comprehensive review and list of resources. *IEEE Geoscience and Remote Sensing Magazine*, *5*(4), 8–36. https://doi.org/10.1109/MGRS.2017.2762307

Foley, J. A., Defries, R., Asner, G. P., Barford, C., Bonan, G., Carpenter, S. R., ... Snyder, P. K. (2005). Global consequences of land use. *Science*, *309*(5734), 570–574. https://doi.org/10.1126/science.1111772

SUPPORTING INFORMATION

Additional supporting information may be found online in the Supporting Information section at the end of the article.